

## Greeks' Sphere: a three-dimensional visualization grammar for financial options

Luís Asiaín<sup>1</sup>, Pedro Pestana<sup>2,3,4</sup>

1 ORCID: 0009-0008-2638-7465 - greekssphere@gmail.com ·

2 Departamento de Ciências e Tecnologia, Universidade Aberta, Lisboa, Portugal (ORCID: 0000-0002-3406-1077) - pedro.pestana@uab.pt

3 Centro de Investigação em Artes e Comunicação (CIAC), Palácio de Ceia, Rua da Escola Politécnica, 147, Lisboa, 1269-001, Portugal

4 CEAUL—Centro de Estatística e Aplicações, Faculdade de Ciências, Universidade de Lisboa, Lisboa, Portugal

### Abstract

We introduce the Greeks' Sphere, a technology-agnostic 3D visualization grammar that unifies the principal option sensitivities—delta ( $\Delta$ ), gamma ( $\Gamma$ ), theta ( $\Theta$ ), and vega ( $v$ )—with strike and time to maturity in a single coherent structure. The scheme is built around an underlying sphere and a cutting plane tied to implied volatility:  $\Delta$  maps to radial wireframe displacement,  $\Gamma$  to smooth procedural mesh undulation (Perlin noise),  $\Theta$  to mesh opacity, and  $v$  to an arc along the cutting section anchored to the plane. A reference prototype instantiates the grammar on option data and enables interactive scans by strike and maturity with stable scales and clearly separated channels, supporting integrated reasoning about multi-Greek behaviour. The prototype exists solely to probe the grammar; implementation choices and data sources are incidental to the model, which is intended to be replicated in other environments. Our contribution is the conceptual grammar itself—transferable across implementation stacks—rather than any specific software artefact.

**Keywords:** financial options; Greeks; implied volatility; 3D visualization; prototypes; human-computer interaction.

**Título:** Esfera das Gregas: uma gramática de visualização tridimensional para opções financeiras

**Resumo:** Apresentamos a Esfera das Gregas, uma gramática de visualização tridimensional agnóstica de tecnologia que unifica as principais sensibilidades das opções — delta ( $\Delta$ ), gamma ( $\Gamma$ ), theta ( $\Theta$ ) e vega ( $v$ ) — com o *strike* e o tempo até à maturidade numa estrutura coesa. O esquema assenta numa esfera de base e num plano de corte associado à volatilidade implícita:  $\Delta$  mapeia-se no deslocamento radial da malha reticular,  $\Gamma$  numa ondulação suave da malha (ruído de Perlin),  $\Theta$  na opacidade da malha e  $v$  num arco ao longo da secção de corte ancorado ao plano. Um protótipo de referência instancia a gramática sobre dados de opções e permite varrimentos interativos por *strike* e maturidade, com escalas estáveis e canais claramente separados, sustentando raciocínio integrado sobre o comportamento multi-gregas. O protótipo existe unicamente para testar a gramática; as escolhas de implementação e as fontes de dados são incidentais ao modelo, que se pretende replicável noutros ambientes. A nossa contribuição é a própria gramática conceptual — transferível entre *stacks* de implementação — e não um artefacto de software específico.

**Palavras-chave:** opções financeiras; gregas; volatilidade implícita; visualização 3D; protótipos; interação homem-máquina.

## 1. Introduction

**Context and motivation:** The options market is a complex domain in which informed decisions require the joint analysis of multiple risk sensitivities—the so-called Greeks ( $\Delta$ ,  $\Gamma$ ,  $\Theta$ ,  $\nu$  [vega])—and their relationship to strike and maturity. Options are versatile instruments that can generate profit even when the underlying price falls, which partly explains their widespread use. Conventional displays present these variables mostly in isolation; to the best of our knowledge, there is no combined, dynamic representation that promotes visual intuition about their joint evolution over the contract's life cycle. In practice, these variables are interdependent and tied to the underlying—particularly to implied volatility—reinforcing the need for an integrated representation. It is therefore pertinent to observe  $\Delta$ ,  $\Gamma$ ,  $\Theta$  and  $\nu$  simultaneously over the life cycle of contracts, preserving proportionality and relationships that isolated 2D widgets rarely make salient.

Given that many transactions in today's financial markets are algorithmic, there is little rationale for a visual artefact intended for machine interpretation. By invoking "intuition," we implicitly restrict the target user to the human agent. A machine ingests raw data and applies algorithms appropriate to the context at hand. A human agent, by contrast, is constrained by emotion, knowledge, and experience. Intuition can be developed with varied tools depending on individual characteristics. Intuition is a distinctly human faculty that should not be underestimated: it synthesizes knowledge, experience, memory, and personality traits into a single mechanism for reasoning and anticipation. A machine can be predictive, but not intuitive; intuition is human. Poorly calibrated intuition, however, can lead to ruin (not only financial). In other words, intuition can be trained, calibrated, and refined. The visual artefact proposed here is intended to support that process and in no case to replace direct decision-making tools.

**Proposal:** The options market is largely non-intuitive, governed by internal mechanisms and rules that only specialized participants fully master. It is an informational ecosystem in which access to and interpretation of data condition positioning and decision-making. Observing these markets can help illuminate dimensions of contemporary economic and political reality, without conferring predictive guarantees. Any participant can buy or sell an underlying asset at a predetermined price by a specified date; the upfront cost corresponds to the option premium. These positions are intrinsically asymmetric: they can cap losses and amplify gains, but the asymmetry can also work against the holder (limited gains with significant losses), contributing to the product's complexity.

The market microstructure depends on real-time data. In many scenarios, the human investor's counterparty is a high-frequency trading (HFT) platform exploiting arbitrage opportunities in milliseconds. A retail investor cannot compete with such systems on speed. Even so, the continued expansion of retail participation calls for tools that enhance understanding and support informed decisions.

Against this backdrop, we propose the Greeks' Sphere, a three-dimensional visual grammar that integrates  $\Delta$ ,  $\Gamma$ ,  $\Theta$ , and  $\nu$  within a cohesive structure built around an underlying sphere and a cutting plane associated with implied volatility. The visual mapping is as follows: mesh radial distance encodes  $\Delta$ ; procedural surface deformation via Perlin noise encodes  $\Gamma$ ; transparency encodes  $\Theta$ ; and an arc drawn on the cutting section encodes  $\nu$ . The aim is to simplify a layer of abstraction, foster users' visual reasoning, and complement—never replace—decision processes.

**Scope and technology neutrality:** We present a reference implementation whose sole purpose is to validate and explore the proposed concept. The current stack (Python/Tkinter for ingestion/export, a WebSocket server for event broadcasting, and a 3D visualization layer in Three.js) was chosen for practical convenience and component availability; it is not a requirement of the model. The Greeks' Sphere is technology-agnostic: it can be replicated in other languages (e.g., C++/Qt, C#/Unity, Java/JavaFX, Rust/WGPU) and web stacks (WebGPU, Babylon.js, etc.), with different client-server architectures (REST, gRPC, pub/sub) and graphics engines, provided the proposed mapping grammar is preserved. Formal user studies with segmented participant groups (retail investors, professional traders, instructors) are deferred to future work, as the artifact's utility is inherently subjective and depends on users' domain literacy, risk tolerance, and psychological factors (§6.3).

With respect to data, the prototype consumes information from a contracted financial telemetry service that offers programmatic access (API) to real-time feeds. For testing, validation, and reproducibility, we also rely on local snapshots adhering to the same data schema. This strategy mitigates common operational constraints (e.g., quotas/rate limits, network-latency variability, provider downtime windows) and enables controlled experiments.

Architecturally, the system is deliberately modular. It separates data acquisition, processing/normalization, and rendering. This separation facilitates portability: swapping the API provider or graphics engine remains straightforward. Maintainability is also preserved—transport protocols, update cadence, or filters can be changed without affecting the conceptual model. In particular, the proposed visualization is not tied to any specific framework or library; such choices are circumstantial, driven by availability and prototyping speed.

Finally, the objectives of this implementation are exploratory and pedagogical: the tool aims to enhance human visual reasoning and support analysis, not to automate investment decisions. The prototype's performance, ergonomics, and operational robustness are discussed only as evidence of feasibility, not as ends in themselves. In production settings, each team may adapt the concept to its technological and regulatory context, in line with internal data policies, compliance, and risk-management practices.

**Objectives:** (i) Transform options data into an intuitive 3D representation; (ii) integrate live data (via API) and enable dynamic exploration by strike and maturity; (iii) formalize and test the Greeks' Sphere grammar; (iv) provide a functional prototype with sliders, play mode, and volume histograms; and (v) discuss limitations (data, rate/pacing limits) and avenues for future work.

## 2. Foundations and State of the Art

### 2.1. Basic concepts and scope

A financial option is a contract that grants its holder the right, but not the obligation, to buy (CALL) or sell (PUT) an underlying asset at a predetermined exercise price (strike) by a specified expiration date (Hull, 2021). The upfront cost paid by the holder is the premium. Over the life of the contract, the relation between the underlying price and the strike yields the usual operational regimes—in-the-money (ITM), at-the-money (ATM), and out-of-the-money (OTM)—which evolve as the market moves and shape the behavior of key risk metrics.

Two exercise styles are common:

- European: exercise is permitted only at maturity.
- American: exercise is permitted at any time up to maturity.

This distinction is primarily relevant for exercise policies and valuation; it is not the focus of this work. For operational reasons related to data availability, the prototype presented here uses American options traded in U.S. markets (e.g., NASDAQ), obtained from a contracted financial-telemetry service with programmatic access to real-time data, complemented—when needed—by equivalent local snapshots. The proposed visual grammar, however, is independent of option style (American/European) and of the data provider.

Within the scope of this article concentrated on computer-engineering aspects—we do not discuss pricing methods nor derive valuation formulas. Our goal is to establish the conceptual basis for visualization: (i) identify the minimal contract elements (underlying, strike, maturity, premium), (ii) understand the role of market conditions (e.g., ITM/ATM/OTM), and (iii) prepare the joint reading of risk variables. The following sections introduce implied volatility—its structure across strike and maturity—and the Greeks whose interdependence motivates a unified three-dimensional representation that facilitates exploratory analysis by human users.

## 2.2. Common representations of options market data

**Two-dimensional options tables (option chains):** The most traditional representation of options market data is the two-dimensional option chain, which organizes contracts by strike and expiration date. Each row typically corresponds to a specific strike, while the left and right halves of the table display call and put contracts, respectively. Alongside quoted prices (bid, ask, and last), the table includes trading volume, open interest, and incremental changes in price. This format offers high analytical precision and compactness, enabling users to identify liquidity concentrations and relative value across strikes. However, despite its quantitative accuracy, the option chain is inherently static and tabular, requiring the user to mentally integrate interrelated variables—such as  $\Delta$ ,  $\Gamma$ ,  $\Theta$ ,  $v$ , and implied volatility—that evolve jointly across both axes of strike and maturity.

While the option chain provides high numerical precision, it places the burden of synthesis entirely on the user: identifying moneyness transitions,  $\Gamma$  peaks, or correlations between Greeks and IV requires effortful cross-referencing across columns. This cognitive load motivates the need for a perceptually integrated representation.

**Two-dimensional Greeks charts:** A common representation of option sensitivities consists of two-dimensional charts in which one of the Greeks—such as Gamma in Figure 2—is plotted against the underlying price or strike. These charts typically display the variation of the selected Greek across the price axis while superimposing additional curves that describe the theoretical profit–loss profile of the position. In the case of Gamma, the curve often peaks around the at-the-money region, reflecting the higher rate of change of Delta near equilibrium, and declines symmetrically as the option moves deeper in- or out-of-the-money. Such 2D representations offer analytical precision and are widely used in trading interfaces, although they remain static and one-dimensional compared with more integrative visual approaches.

AAPL / Option Chain

### Apple Inc. Common Stock (AAPL) Option Chain

Expiration Dates	Option	Strategy	Moneyness	Type
October 2025	Composite	Calls & Puts	Near the Money	All (Types)

Calls							Puts						
Exp. Date	Last	Change	Bid	Ask	Volume	Open Int.	Strike	Last	Change	Bid	Ask	Volume	Open Int.
<b>October 31, 2025</b>													
Oct 31	26.38	+3.63▲	25.45	25.95	25	240	237.50	0.21	-0.15▼	0.20	0.23	662	7856
Oct 31	23.27	+3.33▲	23.10	23.60	531	1990	240.00	0.30	-0.20▼	0.29	0.31	2680	5230
Oct 31	20.89	+2.47▲	20.65	21.35	210	404	242.50	0.43	-0.27▼	0.41	0.44	1506	1480
Oct 31	18.60	+2.50▲	18.45	18.85	165	3877	245.00	0.60	-0.38▼	0.59	0.62	3589	5225
Oct 31	16.59	+3.05▲	16.20	16.60	187	1219	247.50	0.85	-0.50▼	0.85	0.88	971	2777
Oct 31	14.27	+2.51▲	14.15	14.40	1645	7991	250.00	1.22	-0.62▼	1.20	1.25	5872	7298
Oct 31	12.23	+2.34▲	12.15	12.50	593	1495	252.50	1.68	-0.77▼	1.61	1.73	3221	5240
Oct 31	10.38	+2.33▲	10.25	10.50	1331	5913	255.00	2.29	-0.98▼	2.27	2.36	5466	4086
Oct 31	8.60	+1.95▲	8.50	8.85	1907	3009	257.50	3.06	-1.19▼	3.00	3.15	7410	2572
Oct 31	7.05	+1.73▲	7.00	7.25	13496	12035	260.00	4.00	-1.41▼	3.95	4.05	8865	7019
Oct 31	5.65	+1.50▲	5.60	5.75	32920	5677	262.50	5.12	-1.56▼	5.00	5.20	11039	1521
Oct 31	4.45	+1.25▲	4.40	4.55	18828	15698	265.00	6.40	-1.95▼	6.35	6.50	2914	3042
Oct 31	3.50	+1.15▲	3.40	3.50	5155	5713	267.50	7.89	-1.99▼	7.60	8.00	1048	1464
Oct 31	2.63	+0.89▲	2.60	2.68	17587	15622	270.00	9.60	-2.17▼	9.15	10.00	685	6172
Oct 31	1.95	+0.71▲	1.86	2.00	5825	8615	272.50	11.10	-2.45▼	10.90	11.50	573	312
Oct 31	1.43	+0.55▲	1.40	1.45	9672	15146	275.00	13.40	-2.85▼	12.80	13.95	1487	2052
Oct 31	1.02	+0.42▲	1.01	1.05	1774	1597	277.50	14.60	-4.15▼	14.95	15.90	4	62
Oct 31	0.73	+0.29▲	0.73	0.75	4841	9476	280.00	17.60	-4.75▼	17.25	18.10	95	90
Oct 31	0.51	+0.20▲	0.51	0.54	2961	1267	282.50	23.45	--	19.55	20.50	--	6
Oct 31	0.37	+0.15▲	0.36	0.39	1988	3419	285.00	21.96	-5.04▼	21.75	22.95	2	4
Oct 31	0.27	+0.11▲	0.26	0.28	1018	147	287.50	24.40	+0.18▲	24.25	25.40	4	--

LAST TRADE: \$262.82 (AS OF OCT 26, 2025)

Figure 1. 2D options tables



Figure 2. 2D Greeks charts

Two-dimensional Greeks charts excel at displaying the variation of a single sensitivity (e.g.,  $\Gamma$  peaking at ATM), but lack explicit linkage to IV and require toggling between views to reason about multi-Greek scenarios— fragmenting the analytical flow.

**Implied volatility (IV)** is the volatility parameter which, when inserted into a market-accepted option-pricing model, reproduces the observed option price (Gatheral, 2006). It is not directly observable: it is inferred from quotes. In practice, IV provides a summary measure of the market’s perceived uncertainty for a given strike and maturity. By convention, it is reported in annualized terms and depends on the model adopted and trading conditions (liquidity, spreads, trading hours).

**Smile and skew:** Empirically, IV varies with strike, producing the well-known volatility smile (or skew). Some markets exhibit a “smirk” with elevated IV for OTM puts (downside protection), whereas others display a more symmetric curvature (Dupire, 1994). Market state, demand for protection, and the structure of dividends/interest rates influence the shape of the smile. Differences in level and curvature affect the Greeks—particularly vega and delta around ATM.

IV also varies with time to maturity. The term structure may display different slopes (higher short-dated IV under stress; lower in calmer regimes). Examining evolution by days-to-expiration (DTE) helps contextualize regime shifts and interpret changes in sensitivities (e.g.,  $\Gamma$  tends to concentrate in short maturities).

**Volatility surface:** Combining strike and maturity yields the IV surface (strike  $\times$  maturity  $\rightarrow$  IV level). In operational workflows, surfaces are built on discrete grids and completed by interpolation/smoothing (Hagan, Kumar, Lesniewski, & Woodward, 2002) to fill non-quoted points. The surface serves as a reference for calibration, relative pricing, and risk management. From a visualisation standpoint, it is a classic 3D object—but it foregrounds IV alone, hence the need for a unified representation (Sec. 3).

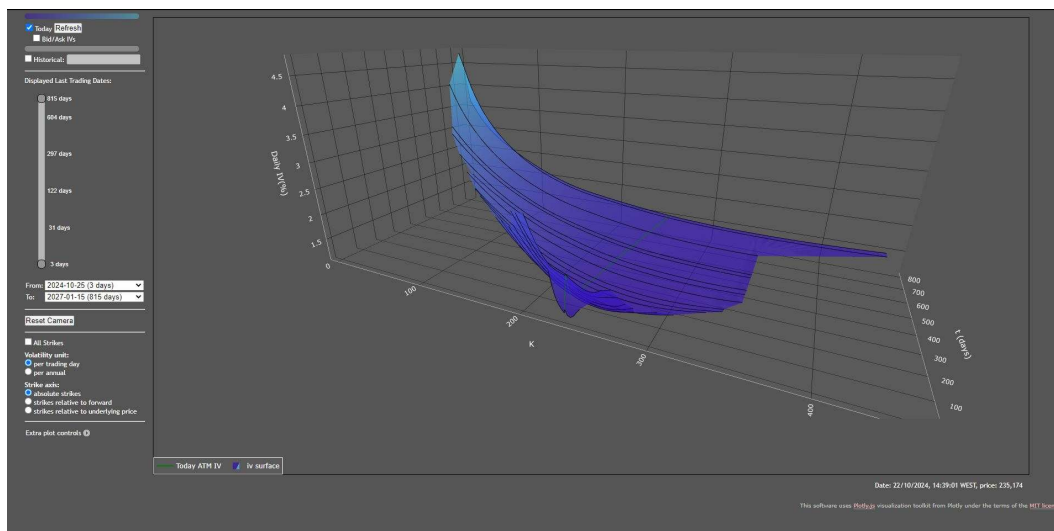


Figure 3. Volatility surface

The volatility surface effectively visualizes the strike × maturity structure of IV but isolates it from the Greeks. To answer questions like "How does vega evolve jointly with this IV contour?" requires mental integration with separate panels—a gap the Greeks' Sphere addresses by co-locating  $v$  with the IV-driven cutting plane.

### 2.3. The Greeks: sensitivities and interdependencies

The Greeks are sensitivity measures of an option's value with respect to its driving variables (underlying price, implied volatility, time to maturity, etc.). They are computed from a market-recognized model and updated continuously by data platforms. In this work we are primarily concerned with their behavior and mutual relations, as these motivate an integrated visualization.

Let:

- P = theoretical option price,
- S = underlying price,
- t = days to maturity,
- $\sigma$  = implied volatility.

The Greeks are then defined as (Hull, 2021):

$$\Delta = \frac{\partial P}{\partial S}, \Gamma = \frac{\partial^2 P}{\partial S^2}, \Theta = \frac{\partial P}{\partial t}, v = \frac{\partial P}{\partial \sigma}.$$

**Delta ( $\Delta$ )** — Sensitivity of the option price to the underlying price.

- Sign and magnitude: CALLs typically have  $\Delta$  in  $[0,1]$ ; PUTs in  $[-1,0]$ .
- Pattern by moneyness: near ATM,  $\Delta$  takes intermediate values; it approaches the extremes ( $\pm 1$ ) in deep ITM and tends to 0 in deep OTM.
- Operational reading: under certain assumptions, approximates the (risk-neutral) probability of expiring ITM; central to hedging.

**Gamma ( $\Gamma$ )** — Curvature of the price–underlying relation, i.e., the rate at which  $\Delta$  changes as the underlying moves.

- Concentration: maximal near ATM and for short maturities; small in deep ITM/OTM.
- Implication: high  $\Gamma$  implies frequent hedge rebalancing ( $\Delta$  changes quickly).

**Theta ( $\Theta$ )** — Sensitivity to the passage of time (time decay). By market convention it is often reported as change per day and is typically negative, especially for OTM/ATM options.

- Typical sign: negative for most options (time value erodes); larger in magnitude near ATM, particularly for short maturities.
- Implication: penalizes strategies reliant on time value; interacts with  $\Gamma$  (short-dated, ATM).

**Vega<sup>1</sup> ( $v$ )** — Sensitivity of the option price to changes in implied volatility; usually positive for both CALLs and PUTs and maximal near ATM.

- Profile: peaks near ATM and tends to fall for very short maturities (less time for uncertainty to realize) and for strikes far from the underlying.
- Implication: shifts in the IV surface transmit directly to option values; key to understanding market shocks.

These quantities are interdependent and modulated by IV, time to maturity, and moneyness, which justifies visualization approaches that integrate the four dimensions simultaneously.

---

<sup>1</sup> "Vega" is not, strictly speaking, a Greek letter; by convention the symbol  $v$  is used (Hull, 2021).

### 3. Methodology / Concept

#### 3.1. Objectives of the artefact

Our proposal seeks to:

- Unify the reading of  $\Delta$ ,  $\Gamma$ ,  $\Theta$ , and  $v$  within a single three-dimensional structure;
- Preserve proportionality and legibility across heterogeneous variables;
- Make relations by strike and maturity salient through controlled scans<sup>2</sup>;
- Foster human visual reasoning while avoiding chromatic overload and ambiguous cues;
- Remain technology-independent (the grammar does not depend on any specific stack).

#### 3.2. Structural elements of the scene

**Underlying sphere:** The sphere is the geometric substrate of the visualization and the reference for the entire construct; its radius sets the baseline scale on which encodings (mesh, deformations, transparencies, and cut) are applied. By convention, the underlying sphere is blue for CALL options and red for PUT options — an arbitrary choice that can be changed at any time.

**Reference axes:** A vertical axis aids the perception of radial displacements ( $\Delta$ ). We also display the positive z-axis, onto which the cutting-plane projection is cast (next item). The remaining axes carry no direct semantics: by construction the sphere is isotropic.

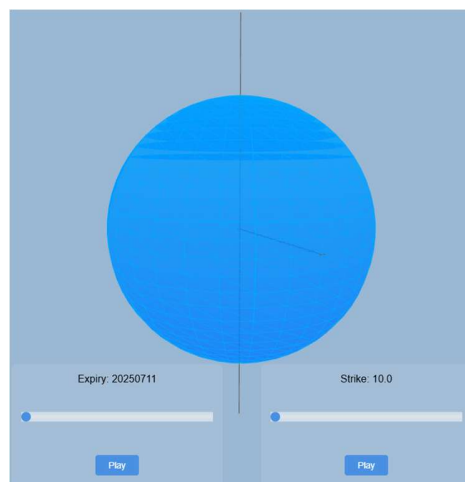


Figure 4. Reference axes

**Cutting plane:** A plane intersects the sphere, generating a circle of intersection. The plane's position is monotonically related to the current implied volatility (IV) of the selected filter (strike/maturity). As the plane advances, the circle's radius and the depth of the cut change accordingly; its value is projected onto the positive z-axis, providing a visual “clock” of IV.

---

<sup>2</sup> In this article, the terms scan and sweep are used interchangeably to refer to the graphical traversal of the option-table's depth levels. Activating any of the “play” controls triggers a sequential visual traversal—effectively a scan or sweep—across the available data contained in the analyzed CSV file.

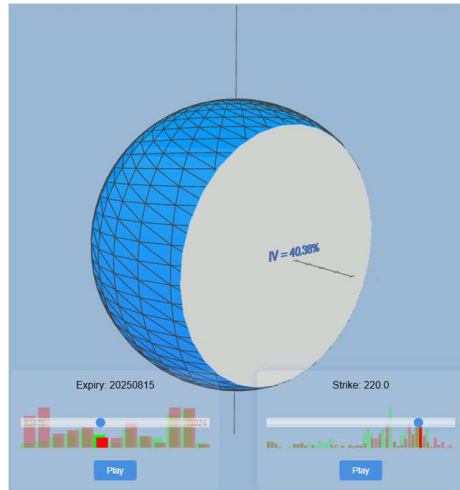


Figure 5. Cutting Plane

### 3.3. Mapping grammar—variable encodings

The grammar assigns each Greek to an explicit visual channel.

$\Delta$  — radial offset of the mesh relative to the underlying sphere.

A wireframe mesh on the sphere shifts outward/inward with  $\Delta$ . The aim is to make the directional contribution of  $\Delta$  visible (movement “away from” or “towards” the center), emphasizing the ATM region where  $\Delta$  changes most rapidly.

**Channel:** radial displacement (magnitude proportional to  $|\Delta|$ ).

**Rationale:** radial distance is an intuitive metric channel for “sensitivity” (Munzner, 2014).

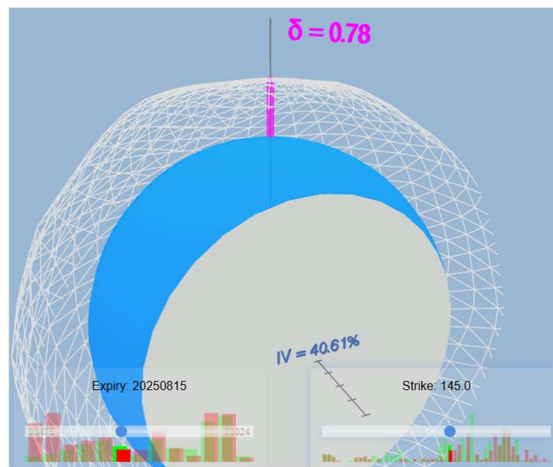


Figure 6. Delta

$\Gamma$  — procedural deformation of the mesh using Perlin noise (Perlin, 1985).

Curvature is encoded as a smooth, persistent undulation whose amplitude increases with  $\Gamma$ —avoiding jitter that could be mistaken for data instability and underscoring that  $\Gamma$  measures how fast  $\Delta$  changes.

**Channel:** deformation amplitude modulated by  $\Gamma$ .

**Rationale:** mesh “ripples” signal local instability in  $\Delta$ -hedging.

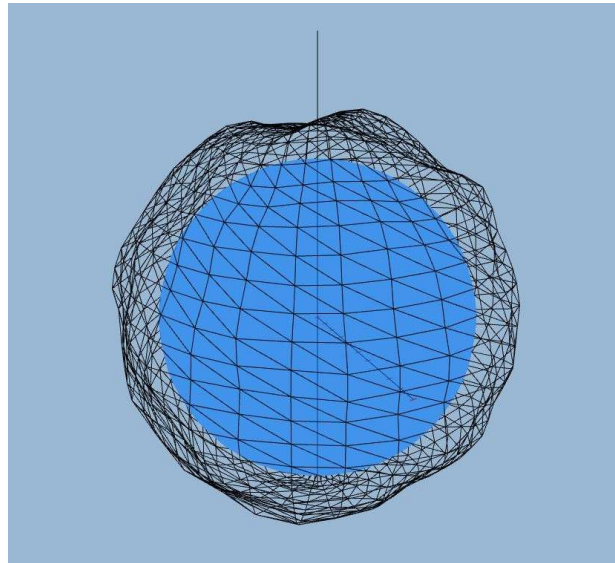


Figure 7. Gamma

$\Theta$  — transparency/opacity of the mesh.

Time-value decay is represented as transparency: larger  $|\Theta|$  (more negative  $\Theta$ )  $\rightarrow$  greater transparency.

**Channel:** alpha/opacity.

**Rationale:** “fading with time” aligns with  $\Theta$ 's semantics.

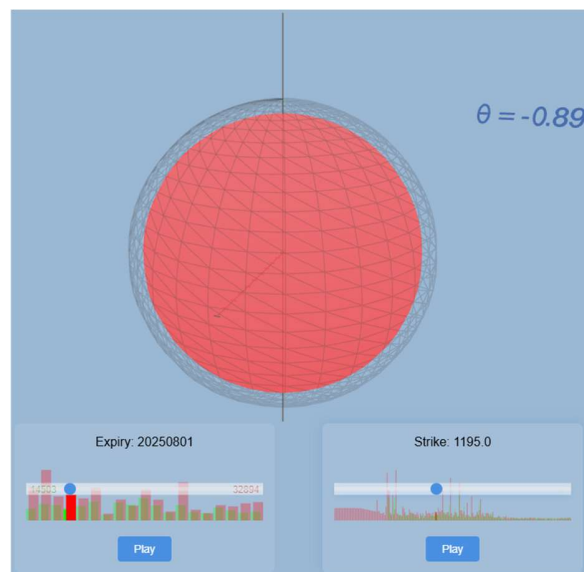


Figure 8. Theta

$v$  — arc on the cutting-circle.

Sensitivity to IV is represented by an arc along the circle of intersection; the arc's length grows with  $v$ . This anchors the reading of  $v$  to the cutting plane (IV), reinforcing their linkage.

**Channel:** arc length.

**Rationale:** avoids contention with  $\Delta/T/\Theta$  on the surface and explicitly ties  $v$  to IV.

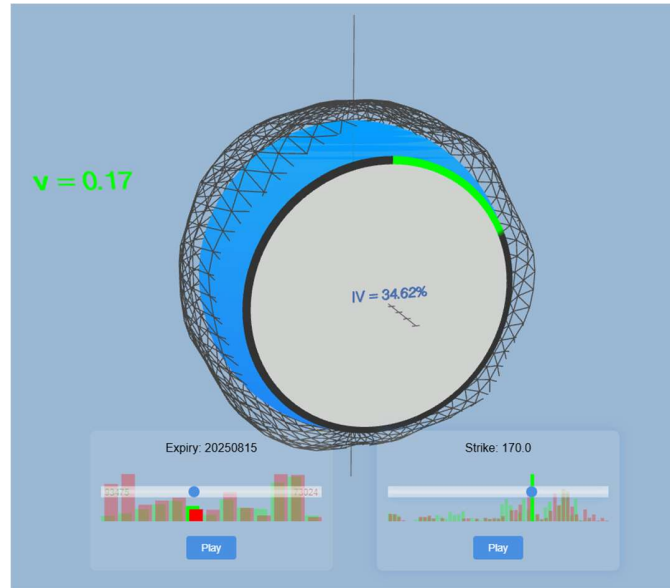


Figure 9. Vega

### ***Moneyness—color encoding***

Moneyness is encoded through the color of the wireframe sphere. The grammar is simple and stable: white denotes ITM, yellow highlights the ATM neighborhood, and black denotes OTM. An achromatic palette with a single chromatic accent (yellow) serves two ends: it maximizes contrast for ITM/OTM against neutral backgrounds and draws attention to the ATM band—where sensitivity typically changes fastest—without competing with the other channels (radial offset, deformation, transparency, and arc).

The width of the “ATM band” is parameterized (a tolerance around moneyness  $\approx 1$ ) and kept constant during sweeps to avoid sudden changes. We also use yellow in the wireframe to toggle the temporary highlighting of  $\Gamma$ . In practice, the yellow corresponding to at-the-money (ATM) is almost imperceptible, since transitions typically occur directly between in-the-money (ITM) and out-of-the-money (OTM) states, with only brief or negligible persistence in the ATM region.

### **3.4. Formal Visual Encoding Specification**

Following Munzner's nested model for visualization design (Munzner, 2014), we formalize the Greeks' Sphere visual grammar through explicit mapping of financial variables to visual channels, considering both perceptual effectiveness and domain-specific semantics. This specification addresses the visual encoding layer of the design space, documenting how abstract data attributes (the Greeks, implied volatility, and moneyness) are translated into retinal variables that support rapid pattern recognition and exploratory analysis.

Table 1 presents the complete encoding specification, integrating data types, visual channels, perceptual effectiveness rankings, design rationales, and implementation parameters employed in the reference prototype.

Table 1. Visual encoding specification

Financial Variable	Data Type	Visual Channel
Delta ( $\Delta$ )	Quantitative	Radial distance of the wireframe mesh relative to the underlying sphere
Gamma ( $\Gamma$ )	Quantitative	Procedural mesh deformation (Perlin noise)
Theta ( $\Theta$ )	Quantitative	Mesh opacity ( $\alpha$ )
Vega ( $v$ )	Quantitative	Arc length on the cutting circle
Implied Volatility (IV)	Quantitative	Cutting-plane position (and z-axis projection), inducing the intersection circle's radius
Moneyness	Categorical	Achromatic color scheme with one yellow accent: white = ITM, yellow = ATM, black = OTM

(Continuation Table 1)

Perceptual Rank	Design Rationale	Parameters / Limits (prototype)
High	Distance/position is the most accurate metric channel for magnitude (sensitivity); emphasizes the ATM region where $\Delta$ changes fastest; a vertical axis aids depth judgement.	Proportional scaling to $ \Delta $ ; stable scales during sweeps; mesh offset is symmetric outward/inward relative to the base sphere.
Medium	Smooth, persistent undulation conveys curvature and local instability in $\Delta$ -hedging; avoids flicker that might be read as data noise.	$\Gamma$ -threshold $\approx 0.001$ ; visual gain = $\min( \Gamma  \times 10, 1) \times 2.0$ ; deformation amplitude capped at $\pm 0.5$ ; when $\Gamma$ is below threshold, geometry is reset to original positions.
Medium	The “fading with time” metaphor matches time decay directly while keeping channels orthogonal to $\Delta/\Gamma/v$ .	opacity = $1 - \min( \Theta , 1)$ ; clamped to $[0, 1]$
High	Anchors vega to the IV plane, thereby avoiding contention on the surface and making the link to implied volatility explicit.	Arc length $\propto v$ ; length scaling preserves monotonicity; co-displayed with the plane's z-projection.

High	Acts as a visual “clock” for IV and a stable reference for $v$ ; mapping is monotonic with the current IV at the selected strike/maturity.	Monotonic mapping with IV; stable scale across sweeps; plane translation governs intersection radius.
High (for categorical discrimination)	Maximizes contrast for ITM/OTM against neutral backgrounds and draws attention to the ATM band without competing with other channels.	Fixed ATM-band tolerance; kept constant throughout sweeps.

### 3.5. Interaction: scans (play buttons) and filters (sliders)

**Scan by strike:** A play control traverses strikes at fixed maturity, animating the grammar and revealing ITM/ATM/OTM transitions,  $\Gamma$  peaks, and variations in  $v$ .

**Scan by maturity:** A second play control traverses expiries at fixed strike, exposing  $\Gamma$ 's concentration at short tenors,  $\Theta$ 's dilution, and  $v$ 's evolution.

**Direct filters:** In both cases, discrete sliders allow manual selection of strike and maturity.

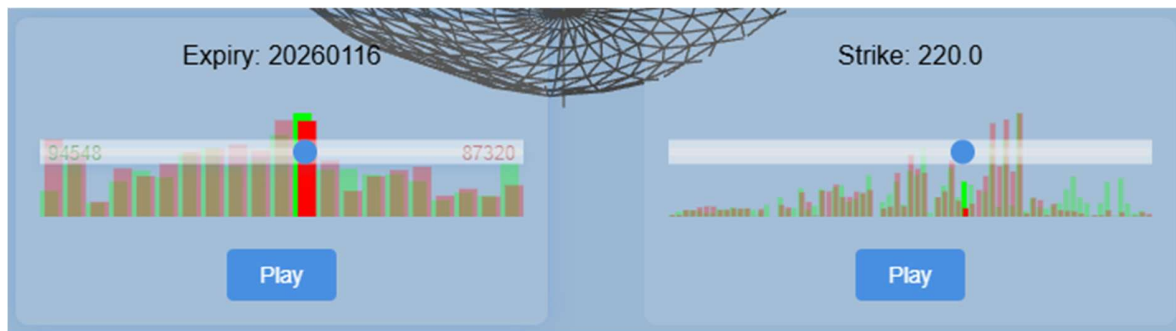


Figure 10. Histograms

For both strike and maturity sweeps, bid/ask volume histograms are overlaid for the relevant dimension. Axis scales remain stable throughout the animation to prevent “ruler changes” that would hinder interpretation.

### 3.6. Data: sources and real-time financial telemetry

The underlying data come from a contracted financial-telemetry service with programmatic access to U.S.-listed American options; when needed, equivalent local snapshots are used for offline exploration and reproducibility. This is a logistical choice and does not constrain the concept: visual grammar is independent of provider and option style. Ingestion retains the essential fields (underlying identifier, strike, expiration date, CALL/PUT type, quoted prices, and computed metrics—implied volatility and the Greeks) and a consistent temporal format across sweeps.

The provider's policy is critical. It is a paid service whose license prohibits redistributing financial data to third parties. Consequently, we cannot publicly release real-time datasets without breaching contractual terms. This restriction is common in market-data services. It

shaped the present design in two ways. First, we prioritize concept demonstration and pipeline documentation. Second, we avoid any mechanism that would turn the prototype into a data-relay channel. The scope of this phase is to prove the concept and lay the foundations for a concrete visual artefact, not to distribute a finished application granting access to financial information. We therefore opted for a sufficient, functional service that enabled experimentation and design development. In future work, adopting a provider with compatible redistribution policies or coupling to public/delayed sources (where available) would allow distributing example datasets with fewer legal constraints, while preserving the solution's technology neutrality and the focus on visual grammar.

### 3.7. Perceptual principles and design choices

The design isolates visual functions.  $\Delta$  uses radial distance;  $\Gamma$ , smooth mesh undulation;  $\Theta$ , transparency; and  $\nu$ , an arc on the IV-driven cut. Each channel is distinct to avoid ambiguity.

To enhance legibility without violating proportionality across variables,  $\Gamma$ 's contribution is presented with a fixed multiplicative scale factor of 10. This choice neither changes ordering nor monotonicity—proportional relations among the Greeks are preserved. It amplifies local curvature so that it becomes discriminable without saturating the scene. Future versions will expose this parameter as user-configurable " $\Gamma$  representation sensitivity" in the range  $[0,10]$ . Zero indicates no amplification; ten indicates the maximum envisaged. This will allow the visual impact of  $\Gamma$  to be tuned to the analytical profile and use context. In the prototype, fixing a single value aims to ensure a harmonious and coherent reading (avoiding aliasing and excessive noise patterns that would arise with very high scaling), consistent with the principles of channel separation, temporal stability, and chromatic parsimony defined for the Greeks' Sphere.

White and black are reserved for moneyness (white/ITM, black/OTM) to avoid overloading the scene; this chromatic economy improves perceptual robustness. Animations favor temporal continuity—without scale or frame jumps—to support trend detection; pausing the scene preserves the same scale.

In summary, the design choices follow three guidelines: (i) a single dominant channel per variable to reduce ambiguity; (ii) stable scales during sweeps to facilitate frame-to-frame comparison; and (iii) chromatic parsimony so that the grammar remains legible, transferable across stacks, and easy for human users to learn.

## 4. Implementation / Reference Prototype

### 4.1. Diagrams of the proposed architecture

#### 4.1.1. Context diagram

The prototype's architecture is organized around a human user—the analyst observing option markets—a desktop configuration/management module, an intermediary server, and a 3D web application (Three.js, 2024) that instantiates the Greeks' Sphere grammar. The analyst interacts with visualization in the browser while, in parallel, configuring parameters and triggering ingestion/export processes via a desktop interface. External connectivity plays two roles: (i) programmatic access (API) to a contracted financial-telemetry service for real-time data; and (ii) rendering in the browser that materializes the 3D scene. This framing clarifies boundaries: the data source is external and replaceable; the conceptual core resides in the web

application and its exploration controls; and the desktop application is not an end-user client but the orchestrator of parameters, processes, and exports.

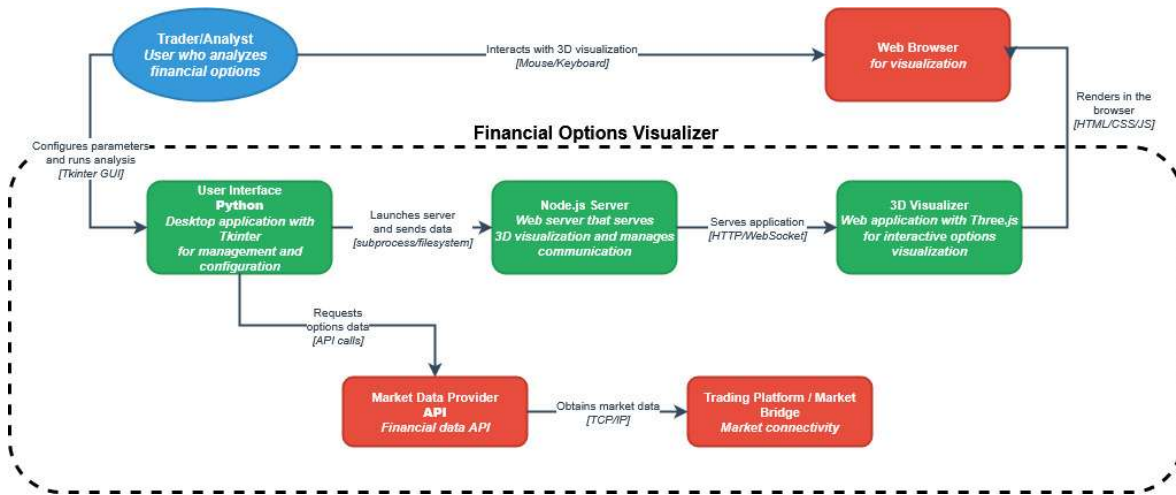


Figure 11. Context diagram

#### 4.1.2. Container diagram

At the container level, the solution explicitly separates data acquisition/preparation, web service, and visualization. The desktop application manages credentials and connections, schedules data requests, and enables bulk exports to local snapshots using the same schema as in real time. The web server exposes an HTTP interface and a WebSocket channel for event broadcasting, loads exported files for offline work, and maintains server-side configuration. The 3D web application coordinates the scene (sphere, cutting plane, wireframe mesh) and manages visualization state and interactions (sweeps, play/pause, filters). This distribution yields two desired properties: portability—any container can be replaced by a technologically different one—and resilience—data-supply issues do not stall the visualization layer nor alter its mapping rules.

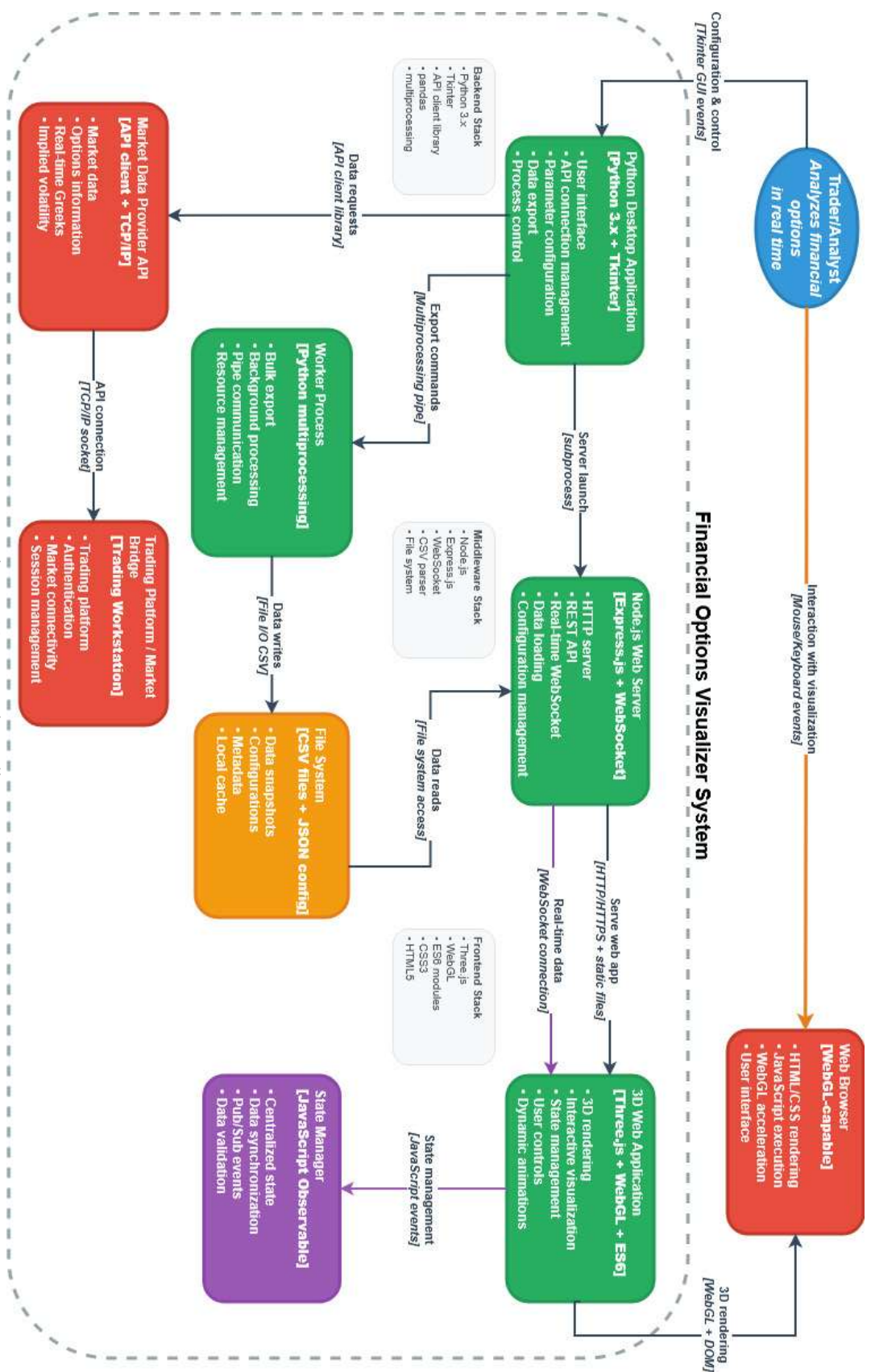


Figure 12. Container diagram

### 4.1.3. Component diagram

At component granularity, the desktop application groups modules for API connection, data collection, processing/validation, and export; the server organizes HTTP and WebSocket handlers, snapshot services, and logging; the 3D application clearly separates scene coordination from the spherical renderer, the cutting-plane/IV module, and the Greeks components (radial offset for  $\Delta$ , deformation for  $\Gamma$ , transparency for  $\Theta$ , and arc for vega), all synchronized by a state manager. This decomposition reduces coupling: the state manager is the single source of truth for scales and normalization; the visual layer is free of transport details; and data services remain independent of graphical-design decisions. The result is a reference prototype that shows how the grammar is instantiated without hard-wiring a mandatory stack.

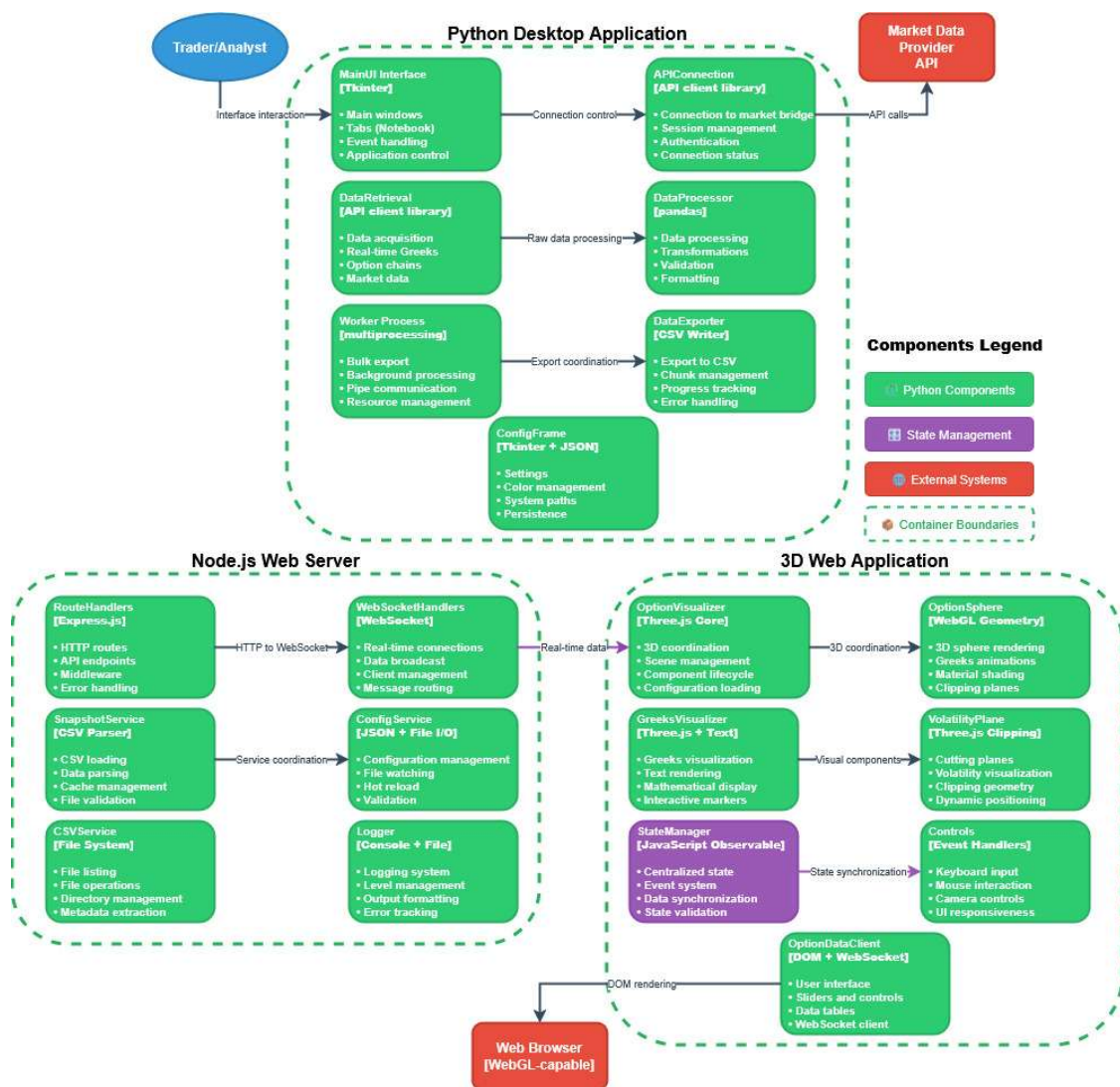


Figure 13. Component diagram

The diagrams support the previously stated principle of technology neutrality: each container can be re-implemented in other ecosystems (languages, 3D engines, protocols). They also make explicit the contractual limit associated with the telemetry provider: the service is paid and does not allow redistribution of data to third parties. Accordingly, the solution prioritizes

documentation of the schema and short video clips demonstrating the sphere operating on real data from local snapshots, thereby avoiding use of the prototype as an unauthorized relay for financial information. The architecture deliberately decouples the grammar from the specific data origin so that readers can reproduce it in their own context under their own license.

#### 4.2. Pipeline and data schema

The pipeline organizes the flow (acquisition → snapshot export → loading → rendering) into decoupled stages. The desktop application connects to the contracted financial-telemetry service, collects option data, and produces CSV snapshots for offline work; the web server loads these files and serves them to the 3D application via HTTP/WebSocket. This design reduces dependence on real-time API latency and enables operation on local snapshots while markets are closed.

The CSV schema used for visualization is stable and easily replicated: it includes underlying identifier, strike, expiration date (DTE), delta, gamma, theta, vega, implied volatility, quoted prices (bid/ask/last), and moneyness class (ITM/ATM/OTM), computed at export time. To reproduce the scene, third parties should generate their own snapshot—with equivalent fields—from a provider with whom they hold a valid license, in compliance with that service’s usage policies.

#### 4.3. Interaction and usage flows

Both sweeps (by strike and by maturity) are retained with play/pause controls, filters, and moneyness encoding in the mesh color (white = ITM, yellow = ATM, black = OTM). To illustrate the behavior of the grammar without redistributing data, the article includes short video clips that show, in particular: (i) a typical OTM→ITM transition during a sweep; and (ii) the joint evolution of  $\Gamma$ ,  $\Theta$ , and  $v$  using real data. The clips were recorded from local snapshots obtained via the API under a valid licence.

#### 4.4. Performance and robustness

The reference prototype incorporates a focused set of design choices that make it robust for controlled testing and subsequent performance measurement:

- **Controlled broadcasting:** The server emits snapshot-load events only when data are valid and coherent; otherwise, it returns an explicit error. This prevents stale states, redundant transfers, and unnecessary recomputation.
- **Client-side state management:** A single source of truth governs scales and normalization. When the scene is paused, scales remain fixed, preserving frame-to-frame comparability and avoiding spurious updates.
- **$\Gamma$  amplitude bounds:** The deformation driven by gamma is subject to a visual cap that suppresses extreme excursions that do not aid interpretation. Proportional ordering is preserved while preventing saturation and aliasing.
- **Back-pressure in acquisition and worker isolation:** Ingestion runs in a background worker with explicit back-pressure (subscriptions are released on completion and producers are signaled under load). Without this multi-process design, a Tkinter-based desktop interface would block during I/O and batch processing.
- **Pacing-aware exporting:** The data exporter implements throttling and accumulation strategies to work around provider-imposed rate/pacing limits—effectively “bypassing” raw API cadence—so acquisition decouples from rendering and local, repeatable runs are enabled.

Together, these measures yield a resilient prototype suitable for experimentation and for the performance analysis reported later.

#### **4.5. Reproducibility and technology neutrality**

The focus at this stage is to demonstrate the concept and document the Greeks' Sphere grammar—not to distribute a finished application with data access. Owing to the provider's contractual conditions (paid service with no permission to redistribute to third parties), neither datasets nor source code (which contains sensitive configuration) are released. Instead, the article provides:

- A formal description of the grammar and visual mappings;
- A specification of the data schema and pipeline (acquisition → snapshot export → loading → rendering), sufficient for readers to generate equivalent snapshots with their own telemetry provider;
- Short video clips with real examples of the sphere's operation, recorded from local snapshots, evidencing the expected grammar behavior in sweeps by strike and by maturity.

This strategy preserves technology neutrality and complies with licensing constraints while providing empirical evidence of the concept and clear guidance for re-implementations across other stacks (languages, 3D engines, protocols).

### **5. Engineering Results and Performance Evaluation**

#### **5.1. Performance and utility assessment**

We identify two key dimensions for assessing the artefact's potential utility: (i) the technical performance of the proposed architecture, and (ii) the practical utility the artefact may—or may not—offer to a human user with varying levels of literacy in options markets.

Psychological factors are central. Two market participants can reach opposite decisions depending on risk tolerance, experience, objectives and personality. This adds uncertainty to any objective assessment of the artefact's utility.

We therefore defer user studies to a later phase. At this stage the goal is to establish conceptual foundations. We describe the architecture of the reference prototype and report technical behavior only to show that the scene can run smoothly at low latency and that each visual element fulfils its intended role. The tool is not designed for automated trading systems; the emphasis here is on human–computer interaction.

Consequently, any user-perceived utility should be assessed via dedicated tests, acknowledging that results will be relatively subjective insofar as they depend, to some extent, on participants' psychology and experience.

With respect to latency, note that financial-telemetry providers may impose different pacing limits on clients to control and moderate access to distributed information. Striving for maximal smoothness, processing data in real time directly via the API inevitably hits the provider's access limits. Internal trials confirm that smooth rendering cannot be sustained when, after a given data volume, the provider applies a timeout as an access-control mechanism.

Naturally, a telemetry provider could enable this sphere in real time directly on its platform without constraints, since it defines the pacing limits for users. A broker could, for example, integrate the sphere into any options table, offering at-a-glance insight into how the table as a whole “breathes.” The goal is to associate the sphere with the table and thereby provide a visual interpretation for data that are typically extensive and abstract—in short, to simplify an abstraction.

Without first-party enablement by a distributor or broker, an individual user should follow this strategy. Access the API during the relevant market's trading hours. Download the full dataset for a given symbol. The intermediate CSV used as an accumulation buffer has 19 columns and an indeterminate number of rows. Row count varies with the availability of option contracts (strikes and expiries). Each row therefore contains 19 fields—the data required to render the Greeks' Sphere. This approach was adopted for the prototype design, while recognizing that the specific stack employed (container diagram §4.1.2) may not be optimal for professional, high-performance environments.

To support evaluation, we implemented a runtime measurement and logging strategy, enabling analysis of performance metrics across multiple examples. We captured five distinct video clips for three listed symbols and published the recordings on YouTube. Each clip's description includes the corresponding performance report, allowing readers to watch the example and inspect the metrics for that specific scene. What follows is an analysis of the recorded data.

## 5.2. Quantitative analysis of the five cases

The table of metrics summarizes five captured scenes for different symbols and option types. In each case, the underlying CSV contains, per snapshot, a number of rows equal to strikes × maturity dates; each row records 19 columns. Thus, even before accounting for temporal evolution, the per-snapshot data volume is substantial—yet the engine sustains fluidity compatible with real-time interaction.

Table 2. Performance metrics<sup>3</sup>

Symbol	Type	Clip Duration (mm:ss)	Snapshot Strikes	Snapshot Maturities	Options in Snapshot	Snapshot Load Time (ms)	Avg FPS
NVDA	CALL	1:43	311	13	4043	1,7	55,61
NFLX	PUT	1:42	406	19	7714	1,3	46,5
GOOGL	PUT	1:57	81	21	1701	0,7	49,91
CSCO	CALL	1:29	51	16	816	0,6	54,1
AAPL	CALL	2:04	102	21	2142	0,9	46,87

<sup>3</sup> Numerical values in Table 2 follow the European decimal notation, using a comma (,) as the decimal separator.

(Continuation Table 2)

Min FPS	Max FPS	FPS Samples	Avg Slider Latency (ms)	Slider Events	Slider Events per min	Avg FPS / 60 (%)
21,63	60,3	534	55,74	469	52,06	92,68
13,46	60	114	58,13	389	200,21	77,5
21,91	60	132	58,48	254	112,49	83,18
22,26	60,1	105	57,75	101	56,43	90,17
20,95	60,1	140	58,6	305	127,53	78,12

**Clip 1: NVDA - CALL - Snapshot 20250707 - Spot 158 USD — 1 min 43 s**

<https://www.youtube.com/watch?v=MWnLLQyDpvY>

CSV volume per snapshot: 4,043 rows × 19 columns = 76,817 fields.

Performance: Avg FPS 55.61 (92.68% of the 60 FPS target), Min 21.63, Max 60.3; FPS samples 534. Snapshot load time 1.7 ms. Avg slider latency 55.74 ms; 469 slider events (52.06/min).

Reading: With ~76k fields per snapshot, the scene holds ~56 FPS—practically indistinguishable from a 60 FPS target.

**Clip 2: NFLX - PUT - Snapshot 20250707 - Spot 1289 USD — 1 min 42 s**

[https://www.youtube.com/watch?v=cR\\_HWOQRmpQ](https://www.youtube.com/watch?v=cR_HWOQRmpQ)

CSV volume per snapshot: 7,714 rows × 19 columns = 146,566 fields.

Performance: Avg FPS 46.5 (77.5%), Min 13.46, Max 60.1; FPS samples 114. Snapshot load time 1.3 ms. Avg slider latency 58.13 ms; 389 events (200.21/min).

Reading: This is the largest per-snapshot volume (~146k fields) and the highest interaction intensity. Even so, the system sustains ~46–60 FPS, preserving scene fluidity.

**Clip 3: GOOGL - PUT - Snapshot 20250707 - Spot 177 USD — 1 min 57 s**

<https://www.youtube.com/watch?v=pMhxnyN5n1E>

CSV volume per snapshot: 1,701 rows × 19 columns = 32,319 fields.

Performance: Avg FPS 49.91 (83.18%), Min 21.91, Max 60.2; FPS samples 132. Snapshot load time 0.7 ms. Avg slider latency 58.48 ms; 254 events (112.49/min).

Reading: With >32k fields per snapshot, the average rate approaches 50 FPS, ensuring smooth transitions and animations.

**Clip 4: CSCO - CALL - Snapshot 20250707 - Spot 68 USD — 1 min 29 s**

<https://www.youtube.com/watch?v=7TzRHKpB5pw>

CSV volume per snapshot: 816 rows × 19 columns = 15,504 fields.

Performance: Avg FPS 54.1 (90.17%), Min 22.26, Max 60.1; FPS samples 105. Snapshot load time 0.6 ms. Avg slider latency 57.75 ms; 101 events (56.43/min).

Reading: With the smallest per-snapshot volume in the set, execution stabilises very near 60 FPS, yielding a particularly fluid visual experience.

**Clip 5: AAPL - CALL - Snapshot 20250707 - Spot 213 USD — 2 min 04 s**

<https://www.youtube.com/watch?v=KM6Z72xvRd0>

CSV volume per snapshot: 2,142 rows × 19 columns = 40,698 fields.

Performance: Avg FPS 46.87 (78.12%), Min 20.95, Max 60.1; FPS samples 140. Snapshot load time 0.9 ms. Avg slider latency 58.6 ms; 305 events (127.53/min).

Reading: With ~41k fields per snapshot, rendering remains above 45 FPS on average, preserving interaction continuity.

Cross-case synthesis:

- Per-snapshot volume ranges from 15,504 to 146,566 fields.
- Snapshot load time remains  $< 2$  ms in all scenarios, indicating that local ingestion is not a limiting factor.
- Avg slider latency is  $\approx 58$  ms (mean  $\approx 57.74$  ms), supporting a perception of immediate response.
- Global avg FPS is  $\approx 50.6$  FPS ( $\approx 84.3\%$  of a 60 FPS target), with peaks near 60 FPS and brief dips concentrated in the most interaction-intensive/complex scenes.

**Conclusion:** Even when accessing high per-snapshot volumes—tens to hundreds of thousands of fields—the pipeline delivers the required scene fluidity, with low load latency and consistent response times during interactive manipulation. These observations support the suitability of the architecture for near-real-time representation of extensive, abstract options tables<sup>4</sup>.

### 5.3. Notes on interdependencies and typical patterns observed

**By moneyness (fixed maturity).**

- Approaching ATM:  $\Gamma$  increases (Perlin undulation),  $v$  rises (greater sensitivity to IV),  $\Theta$  becomes more negative (stronger time decay), and  $\Delta$  transitions rapidly from low (OTM) to high (ITM) values.
- Deep ITM:  $\Delta$  saturates ( $\approx \pm 1$ );  $\Gamma$  and  $v$  become small;  $\Theta$  is often less penalising per unit time.
- Deep OTM:  $\Delta$  tends towards 0;  $\Gamma$  and  $v$  are reduced;  $\Theta$  may be small in absolute terms yet material in relative terms (value is mostly time value).

**By maturity (fixed moneyness).**

- Short-dated:  $\Gamma$  and  $|\Theta|$  tend to increase around ATM;  $v$  tends to fall (little time for uncertainty to realise).
- Long-dated:  $v$  increases (greater exposure to IV shifts);  $\Gamma$  smooths;  $\Theta$  is diluted over a longer horizon.

With this artefact, users can visually explore an options table in its entirety along two axes of analysis: strike and expiration date. The “underlying sphere” provides the permanent structural reference for the scene; the remaining variables are mapped around it using values obtained from the financial-telemetry service. This fixed sphere encodes the value of the underlying asset and serves as a visual anchor. From it, a proportionality and referencing scheme is established that ensures graphical coherence among all elements. Once the encoding rules and the sphere’s design are internalized, the relationships among components become immediate, enabling consistent navigation across the table’s two axes (strikes  $\times$  maturities).

---

<sup>4</sup> All performance tests were conducted on a workstation equipped with an Intel Core i9-14900K processor, 64 GB RAM, and an NVIDIA T1000 GPU (8 GB VRAM)

## 6. Related Work: alternatives comparison

### 6.1. Analytic task set and weights

#### Tasks T1 – T5

- T1 — OTM→ATM→ITM transition salience. Ability to detect moneyness transitions as the scan moves across strikes/expiries.
- T2 —  $\Gamma$  peak localization near ATM. Ability to identify where curvature concentrates (typically around ATM, especially for short tenors).
- T3 —  $v$  estimation explicitly tied to IV. Ability to read vega in a way that is explicitly anchored to the current level of implied volatility.
- T4 —  $\Theta$  reasoning without channel collisions. Ability to reason about time decay ( $\Theta$ ) without overloading or confounding other channels.
- T5 — Stable navigation of the strike  $\times$  maturity grid. Ability to traverse the option table (by strike or maturity) with stable scales and coherent feedback.

Weights: We adopt  $w = [0.25, 0.25, 0.20, 0.15, 0.15]$  for [T1, T2, T3, T4, T5].

Rationale: ATM transitions (T1) and  $\Gamma$  peaks (T2) are central to risk intuition;  $v$  tied to IV (T3) is next in importance;  $\Theta$  and scan ergonomics (T4–T5) remain essential but slightly less critical.

### 6.2. Task-adequacy rubric (1-5) with weighted score

Approaches compared: Volatility surface; Two-dimensional Greeks chart (single sensitivity plotted in 2D; e.g.,  $\Delta$  or  $\Gamma$  vs strike/underlying); 2D options table (option chain); Greeks’ Sphere.

Table 3. Task-adequacy rubric and weighted score

Approach	T1	T2	T3	T4	T5	Weighted score
Volatility surface	2	1	2	1	4	1,90
2D Greeks chart	4	4	3	3	3	3,50
2D options table	3	2	3	3	4	2,90
Greeks’ Sphere	5	4	5	4	4	4,45

#### 6.2.1. Justification of the scores:

##### Volatility surface

T1 = 2: Moneyness must be inferred indirectly; the surface encodes implied volatility only.

T2 = 1: Gamma is not represented; curvature in the price–underlying relation is absent.

T3 = 2: Vega is not encoded explicitly; any inference is indirect from IV curvature.

T4 = 1: Theta is not represented.

T5 = 4: The 3D surface covers the strike $\times$ maturity space well but foreshortening and occlusion reduce precision.

##### Two-dimensional Greeks chart

T1 = 4: Delta plots make the ATM transition visually explicit, though each Greek requires a separate view.

T2 = 4: Gamma versus strike clearly exposes ATM concentration through a visible curve peak.

T3 = 3: Vega curves can be plotted but are not inherently linked to the instantaneous IV level unless manually overlaid.

T4 = 3: Theta curves are legible and isolated; however, switching between Greeks may interrupt continuity.

T5 = 3: Each chart generally depicts one dimension (strike or underlying); navigating both strike  $\times$  maturity requires separate charts or reconfiguration.

### 2D options table

T1 = 3: A moneyness column aids classification, yet transitions are numerical rather than perceptual.

T2 = 2: Gamma peaks are difficult to identify without additional visual encoding such as color intensity.

T3 = 3: Vega and IV columns can be compared, though the relation is numeric, not visual.

T4 = 3: Theta is accessible as a value but lacks a perceptual metaphor; channel collisions are minimal.

T5 = 4: The table covers the full strike  $\times$  maturity grid and remains stable, but interpretation depends on textual scanning rather than visual continuity.

### Greeks' Sphere

T1 = 5: Moneyness is encoded through an achromatic palette, while Delta is mapped to radial distance—together making OTM $\rightarrow$ ATM $\rightarrow$ ITM transitions highly salient during strike scans.

T2 = 4: Gamma is represented by smooth procedural undulation using Perlin noise; this medium-strength channel conveys local curvature effectively without producing jitter.

T3 = 5: Vega is shown as an arc length along the cutting circle, explicitly anchored to the IV plane, ensuring a direct and interpretable link between  $v$  and IV.

T4 = 4: Theta is mapped to opacity, a metaphor semantically faithful to time decay.

T5 = 4: Both strike and maturity scans maintain fixed scales and stable histograms, supporting coherent traversal; minor 3D occlusion limits the score to 4 rather than 5.

**Comparative assessment:** We position the Greeks' Sphere within the broader design space of option-analytics visualization by contrasting it with volatility-surface plots, two-dimensional Greeks charts, and conventional option-chain tables. Traditional interfaces tend to isolate each sensitivity— $\Delta$ ,  $\Gamma$ ,  $\Theta$ ,  $v$ —into separate widgets or columns, hindering integrated reasoning.

An analytic task-adequacy rubric (T1–T5; 1–5 scale; weights 0.25/0.25/0.20/0.15/0.15) yields a weighted score<sup>5</sup> of 4.45 / 5 for the Greeks' Sphere, compared with 1.90 – 3.50 for alternative approaches. The results are consistent with the expected advantages of metric channels for  $\Delta$  and  $v$ , the semantic match of opacity for  $\Theta$ , and the explicit IV anchor provided for  $v$ .

#### 6.2.2. Comparative matrix

The comparative matrix reveals a design-space trade-off. Traditional approaches optimize for specific strengths:

- Volatility surfaces for IV-centric analysis with minimal cognitive load
- 2D Greeks charts for high-precision single-Greek inspection
- 2D tables for comprehensive numerical coverage

---

<sup>5</sup> These scores reflect an analytical, perception-based evaluation of representational adequacy rather than an empirical user study. They provide a conceptual benchmark for future empirical validation involving time-to-insight and error-rate measurements.

The Greeks' Sphere occupies a distinct niche: it sacrifices some numerical precision (inherent in 3D occlusion) in exchange for perceptual integration— enabling at-a-glance pattern detection across  $\Delta/\Gamma/\Theta/v$  and their joint evolution with IV. This makes it complementary rather than substitutive: users would typically employ the sphere for exploratory pattern identification, then revert to traditional tools for precise quantitative analysis (§6.3).

Table 4. Comparative matrix

Approach	Variables covered	Primary encodings	Interaction model	2D/3D
Volatility surface	IV only ( $\Delta/\Gamma/\Theta/v$ separate)	Mesh height/position on strike×maturity grid	Rotate/zoom; cross-hair	3D
2D Greeks chart	One Greek at a time (toggle)	Line/area vs strike or underlying	Pan/zoom; overlay/toggle	2D
2D options table	$\Delta, \Gamma, \Theta, v, IV$ (numeric)	Tabular values; conditional formatting	Sorting/filtering; paging	2D
Greeks' Sphere	$\Delta, \Gamma, \Theta, v + IV$	$\Delta \rightarrow$ radial, $\Gamma \rightarrow$ undulation, $\Theta \rightarrow$ opacity, $v \rightarrow$ arc linked to IV, IV $\rightarrow$ cutting plane	Strike/maturity scans (play), sliders, volume histograms; stable scales	3D

(Continuation Table 4)

Integrated $\Delta/\Gamma/\Theta/v$	Scalability / performance	Reproducibility	Typical limitations
No (IV isolated)	High (interpolated grids)	Widely available	Shows only IV; 3D occlusion; does not expose Greeks jointly.
Partial (single-channel)	High	High	Fragmented reading; linking to IV is indirect; needs toggling for multi-Greek context.
Partial (numeric juxtaposition)	High	High	Dense; limited perceptual salience; cross-dimensional patterns are effortful to spot.
Yes (single grammar)	~50–56 FPS avg; slider latency $\approx 58$ ms; snapshot load $< 2$ ms (prototype)	Stack-agnostic, modular; snapshots for reproducibility	3D occlusion (managed); short learning curve.

### 6.3. Limitations and Future Work

At this stage of our exposition and analysis, it is important to stress that our thesis is not intended to replace existing graphical representations but to complement them. We have compared our proposal with commonly used alternatives without diminishing their utility or relevance—each has an undisputed context of use. Nothing surpasses the precision of a two-dimensional options table. Our contribution, however, offers an additional—rather than substitutive—capability: it condenses, within a single dynamic graphical structure, the behavior and interplay of several (intrinsically abstract) variables across their two principal depth axes, namely all available strikes and maturity dates. The sphere yields a dynamic

image whose motion is useful for identifying regions of interest and trends. Once such regions are identified, a prospective user can revert to their customary tools and workflows. In short, the artefact is an auxiliary aid; it is not a tool whose nature is to prescribe concrete trading decisions.

We have sought to motivate, in a systematic manner (see §3.4 Table 1 p.12), the design choices underlying the mapping of variables to their respective elements in the scene. The rationale for these choices is laid out, while acknowledging that other, equally defensible mappings could have been adopted. In any case, the proposal is thus defined.

Other variables were deliberately left outside this first iteration. Quantities such as rho, vanna, zomma, vomma, veta, charm, among others, could be mapped to additional channels within the artefact. At this stage, however, their inclusion would introduce undue complexity into an initial prototype whose purpose is to establish the conceptual foundations of an alternative representation for this already complex and abstract class of financial information. We contend that the elements treated here provide the basis for a concrete representational structure from which future extensions may develop. Attempting to map every available variable merely for the sake of completeness (or near-completeness) would likely prove counterproductive. The objective is to assist the human agent in interpreting large volumes of options data and to offer a new orienting, interpretive modality; designing a tool that complicates, rather than simplifies, this abstraction would be at cross-purposes with that aim. With the proposed design, one can visually apprehend how a given two-dimensional options table “breathes.” That, at least, is our intention.

As future work, we plan to design user studies to assess the artefact’s practical utility, the learning curve across user groups with heterogeneous prior knowledge, and any real-world applications suggested by those results. Because recruiting the intended target profile — a technically skilled user who already brings domain familiarity—is non-trivial, we envisage hybrid outreach that combines social-media dissemination with academic channels to circulate screening questionnaires and collect structured feedback from qualified participants. In parallel, we will evaluate the artefact’s impact on non-professional audiences to gauge its suitability as an educational resource.

## 7. Conclusion

We propose a three-dimensional, dynamic artefact for the graphical interpretation of risk in options analysis via the Greeks. We formalize a visual grammar that maps these variables to distinct channels within a 3D scene and motivates the corresponding design choices. On this basis, we developed a reference prototype to prove the grammar’s usefulness; the architecture adopted here is contingent and chosen for convenience, and the artefact can be replicated in other languages and frameworks provided the mapping rules are preserved. Our effort in this phase prioritized the grammar and a prototype sufficiently established the concept. We introduced internal design mechanisms to work around operational constraints encountered during development (e.g., broker pacing/policy timeouts) and instrumented the system to measure runtime performance. Given licensing constraints of the financial-telemetry service, we publish representative captures with their performance reports so readers can judge both the visual effect and runtime characteristics (reports are linked in each video’s description; see §5.2, Table 2). We also defined a task-based rubric to compare the artefact with alternative visualizations; results are favorable but should be read in context—each alternative is

optimized for its own use case, and it is expected that our artefact scores highest in the setting for which it was designed.

The options market remains a domain where information asymmetry and cognitive complexity create barriers to entry. By transforming abstract numerical tables into a visually integrated "breathing" structure, the Greeks' Sphere reduces one layer of abstraction—not to replace decision tools, but to augment human intuition in a market increasingly dominated by algorithmic actors. The grammar's technology neutrality ensures it can evolve alongside the ecosystem it seeks to illuminate.

**Acknowledgments.** This work was supported by FCT — Fundação para a Ciência e a Tecnologia, Portugal, under project UID/04019/2025

## REFERENCES

Black, F., & Scholes, M. (1973). The Pricing of Options and Corporate Liabilities. *The Journal of Political Economy*, 81(3), 637–654. doi:10.1086/260062

Cox, J. C., Ross, S. A., & Rubinstein, M. (1979). Option Pricing: A Simplified Approach. *Journal of Financial Economics*, 7(3), 229-263. doi:10.1016/0304-405X(79)90015-1

Derman, E., & Kani, I. (1994). Riding on a Smile. *RISK*, 7(2), 32-39.

Dupire, B. (1994). Pricing with a Smile. *RISK*, 7(1), 18-20.

Gatheral, J. (2006). *The Volatility Surface: A Practitioner's Guide*. New York: Wiley. doi:10.1002/9781119202073

Hagan, P. S., Kumar, D., Lesniewski, A. S., & Woodward, D. E. (2002). Managing Smile Risk. *Wilmott*, 84-108.

Heston, S. L. (1993). A Closed-Form Solution for Options with Stochastic Volatility with Applications to Bond and Currency Options. *The Review of Financial Studies*, 6(2), 327-343. doi:10.1093/rfs/6.2.327

Hull, J. C. (2021). *Options, Futures, and Other Derivatives (11th ed.)*. London: Pearson.

Merton, R. C. (1973). Theory of Rational Option Pricing. *The Bell Journal of Economics and Management Science*, 4(1), 141-183. doi:10.2307/3003143

Munzner, T. (2014). *Visualization Analysis and Design*. Boca Ratón: A K Peters / CRC Press. doi:10.1201/b17511

Perlin, K. (1985). An Image Synthesizer. *ACM SIGGRAPH Computer Graphics*, 19, pp. 287-296. doi:10.1145/325165.325247

Three.js, A. (2024). *Three.js documentation (r180)*. Retrieved 2024, from <https://threejs.org/>

Ware, C. (2020). *Information Visualization: Perception for Design (4th ed.)*. Cambridge, MA: Morgan Kaufmann.



**Luís Asiaín** holds a BSc in Informatics Engineering (Computer Science) from Universidade Aberta (UAb), completed in 2025. The author is currently employed at the Spanish Ministry of Foreign Affairs, European Union and Cooperation (Ministerio de Asuntos Exteriores, Unión Europea y Cooperación) in its representation in Lisbon, Portugal. This article derives from the presentation and defense of the undergraduate capstone project and has been prepared independently; the author has no affiliation with any financial institution or investment platform.



**Pedro Duarte Pestana** holds a PhD in Music Informatics from the Catholic University of Portugal. He serves as an Assistant Professor in the Section of Informatics, Physics and Technology (SIFT) at Universidade Aberta since 1 March 2022. His work lies at the intersection of multimedia signal processing and the perception and cognition of auditory and visual phenomena. He has worked as a consultant for several international signal-processing software companies and contributed to the formation of a Montreal-based startup focused on artificial-intelligence systems for audio processing. He publishes regularly in venues such as the Audio Engineering Society, DAFx and ISMIR, for which he is also an active reviewer and member. He is Portugal's national representative for ISO/TC 43/SC 1. He was the recipient of a Gulbenkian Professorship between 2015 and 2019 and served as Director of the Research Centre for Science and Technology of the Arts (CITAR), where he is currently a collaborating researcher. He is also an integrated researcher at the Research Centre for Arts and Communication – Universidade Aberta (CIAC-UAb). CiênciaVitae: <https://www.cienciavitae.pt/portal/2714-8A7B-5CCA>